Received: 15 February 2019 | Accepted: 12 August 2019

DOI: 10.1002/hyp.13571

RESEARCH ARTICLE

WILEY

Moisture origin and stable isotope characteristics of precipitation in southeast Siberia

Svetlana S. Kostrova[1,2] | Hanno Meyer[2] | Francisco Fernandoy[3,4] | Martin Werner[5] | Pavel E. Tarasov[6]

[1]A.P. Vinogradov Institute of Geochemistry, Siberian Branch of Russian Academy of Sciences, Irkutsk, Russia

[2]Alfred Wegener Institute Helmholtz Centre for Polar and Marine Research, Research Unit Potsdam, Potsdam, Germany

[3]Facultad de Ingeniería, Laboratorio de análisis isotópico, Universidad Andrés Bello, Viña del Mar, Chile

[4]Centro de Investigación para la Sustentabilidad, Universidad Andrés Bello, Santiago, Chile

[5]Alfred Wegener Institute Helmholtz Centre for Polar and Marine Research, Bremerhaven, Germany

[6]Institute of Geological Sciences, Palaeontology, Freie Universität Berlin, Berlin, Germany

Correspondence
Svetlana S. Kostrova, A.P. Vinogradov Institute of Geochemistry, Siberian Branch of Russian Academy of Sciences, Favorsky Str. 1a, 664033 Irkutsk, Russia.
Email: kostrova@igc.irk.ru; svetlana.kostrova@awi.de

Funding information
BMBF, Grant/Award Number: 03G0859; SSHRC, Grant/Award Number: 895-2018-1004; Ministry of Education and Science of the Russian Federation, Grant/Award Number: IGC SB RAS IX.127.1.2

Abstract

The paper presents oxygen and hydrogen isotopes of 284 precipitation event samples systematically collected in Irkutsk, in the Baikal region (southeast Siberia), between June 2011 and April 2017. This is the first high-resolution dataset of stable isotopes of precipitation from this poorly studied region of continental Asia, which has a high potential for isotope-based palaeoclimate research. The dataset revealed distinct seasonal variations: relatively high $\delta^{18}O$ (up to −4‰) and δD (up to −40‰) values characterize summer air masses, and lighter isotope composition (−41‰ for $\delta^{18}O$ and −322‰ for δD) is characteristic of winter precipitation. Our results show that air temperature mainly affects the isotope composition of precipitation, and no significant correlations were obtained for precipitation amount and relative humidity. A new temperature dependence was established for weighted mean monthly precipitation: +0.50‰/°C (r^2 = 0.83; p <.01; n = 55) for $\delta^{18}O$ and +3.8‰/°C (r^2 = 0.83, p < 0.01; n = 55) for δD. Secondary fractionation processes (e.g., contribution of recycled moisture) were identified mainly in summer from low d excess. Backward trajectories assessed with the Hybrid Single-Particle Lagrangian Integrated Trajectory (HYSPLIT) model indicate that precipitation with the lowest mean $\delta^{18}O$ and δD values reaches Irkutsk in winter related to moisture transport from the Arctic. Precipitation originating from the west/southwest with the heaviest mean isotope composition reaches Irkutsk in summer, thus representing moisture transport across Eurasia. Generally, moisture transport from the west, that is, the Atlantic Ocean predominates throughout the year. A comparison of our new isotope dataset with simulation results using the European Centre/Hamburg version 5 (ECHAM5)-wiso climate model reveals a good agreement of variations in $\delta^{18}O$ (r^2 = 0.87; p <.01; n = 55) and air temperature (r^2 = 0.99; p <.01; n = 71). However, the ECHAM5-wiso model fails to capture observed variations in d excess (r^2 = 0.14; p < 0.01; n = 55). This disagreement can be partly explained by a model deficit of capturing regional hydrological processes associated with secondary moisture supply in summer.

KEYWORDS
atmospheric circulation, Baikal region, d excess, ECHAM5-wiso climate model, HYSPLIT model, stable oxygen and hydrogen isotopes of precipitation

1 | INTRODUCTION

Climate change and its impacts on weather conditions and ecosystems at the global and regional scale has become an important issue for science, economy, and politics in recent decades (Intergovernmental Panel on Climate Change, 2014). Changes in atmospheric circulation regimes are particularly important, as these primarily control directions and seasonal distribution of moisture transporting air masses, and, consequently, determine regional water budgets (Harrison, Yu, & Tarasov, 1996) and atmospheric precipitation sources (e.g., Osipova & Osipov, 2016). Climate proxy records (e.g., pollen, diatoms, and stable isotopes) derived from sedimentary archives worldwide play an important role in reconstructing past changes in atmospheric circulation and precipitation, thus extending our knowledge beyond the relatively short interval covered by instrumental measurements and satellite data.

Atmospheric precipitation is the primary source of water for terrestrial and aquatic ecosystems (Brázdil, 1992; Galloway & Cowling, 1978). Hence, the detailed understanding of circulation processes and background mechanisms controlling precipitation of a given region and its temporal and spatial variations is an important issue for assessment and forecast of weather and water regimes worldwide (Bailey, Klein, & Welker, 2019; Brázdil, 1992; Tang et al., 2017; Trenberth, 2011). In particular, hydrogen and oxygen isotopes in precipitation are natural tracers, which help to understand the atmospheric moisture cycle (Araguás-Araguás, Froehlich, & Rozanski, 2000). Variations in stable isotope composition (δD and δ^{18}O) of precipitation are caused by isotope fractionation processes occurring at phase transitions in the hydrological cycle (Dansgaard, 1964). They correlate with climatic parameters such as air temperature, humidity, and precipitation amount (Dansgaard, 1964; Rozanski, Araguás-Araguás, & Gonfiantini, 1993) and are defined by air mass trajectories (Kurita, 2011; Merlivat & Jouzel, 1979). Consequently, stable isotopes have a great potential to provide unique information on atmospheric circulation patterns and climate changes. In recent years, the stable isotope composition of precipitation has become one of the most reliable tools for meteorological, climatological, and hydrological studies (Bowen, 2010; Tang et al., 2017; Wei, Lee, Liu, Seeboonruang, & Koike, 2018; Wu, Zhang, Xiaoyan, Li, & Huang, 2015; Yang et al., 2019) and modelling (Bowen, 2008; Butzin et al., 2014; Gryazin et al., 2014; Werner, Langebroek, Carlsen, Herold, & Lohmann, 2011; Yao et al., 2013). In addition, data on isotope composition of modern precipitation are widely used for decoding information about past climate conditions stored in natural archives (Rozanski, Johnsen, Schotterer, & Thompson, 1997) such as lake sediments (Kostrova, Meyer, Chapligin, Tarasov, & Bezrukova, 2014; van Hardenbroek et al., 2018), ground ice (Meyer et al., 2015; Meyer, Dereviagin, Siegert, Hubberten, & Rachold, 2002), firn/ice cores (Casado, Orsi, & Landais, 2017; Fernandoy, Meyer, & Tonelli, 2012; Pang, Hou, Kaspari, & Mayewski, 2014), tree rings (e.g., Leonelli et al., 2017), and cave stalagmites (Liang et al., 2015; Partin et al., 2012).

The data gathered over the last six decades by the Global Network of Precipitation (GNIP) of the International Atomic Energy Agency (IAEA) and the World Meteorological Organization (WMO) are supplemented by numerous local studies to provide a detailed picture of the spatial and temporal variability of the isotopic composition of precipitation worldwide. However, stable isotope data of precipitation from the vast area of Russia are sparse and often discontinuous (International Atomic Energy Agency/World Meteorological Organization [IAEA/WMO], 2018). Meteorological and stable isotope data from 13 stations across Russia (summarized in the Siberian Network for Isotopes in Precipitation) were analysed for reconstructing spatial and temporal variations in isotopic composition of precipitation (Chizhova et al., 2016; Kurita, 2011; Kurita et al., 2005; Kurita, Numaguti, Sugimoto, Ichiyanagi, & Yoshida, 2003; Kurita, Yoshida, Inoue, & Chayanova, 2004; Malygina, Eirikh, Kurepina, & Papina, 2019; Papina, Malygina, Eirikh, Galanin, & Zheleznyak, 2017). These studies point to the significance of the moisture transport from the Atlantic Ocean (especially in winter) and the contribution of recycled water (i.e., convective rains falling in summer) in the continental interior of Eurasia. However, these conclusions are based on the currently available data, in which the entire Baikal region (southeast Siberia) is represented by an incomplete, single-year record of monthly mean isotope data from Irkutsk (IAEA/WMO, 2018).

The Baikal region with approximately 3.5 million inhabitants is one the most populated and economically important areas of Siberia. Since the 1990s, the region has increasingly become a centre of palaeoenvironmental studies using sedimentary archives from Lake Baikal (Kravchinsky, 2017; Kuz'min, Khursevich, Prokopenko, Fedenya, & Karabanov, 2009) and numerous small lakes (Bezrukova, Tarasov, Solovieva, Krivonogov, & Riedel, 2010; Danilenko, Solotchin, & Solotchina, 2015; Leonova et al., 2018; Mackay, Bezrukova, et al., 2013; Sklyarov et al., 2010). In particular, oxygen isotope records from diatoms (Kalmychkov, Kuz'min, Pokrovskii, & Kostrova, 2007; Kostrova et al., 2013, 2014, 2016; Mackay et al., 2011, Mackay, Swann, et al., 2013; Morley, Leng, Mackay, & Sloane, 2005; Swann et al., 2018) and ostracods (Tarasov et al., 2019) have been analysed and demonstrate the relationship between isotope signals preserved in sedimentary archives and ancient atmospheric precipitation patterns. All these studies require the knowledge of the stable isotope composition of recent regional precipitation. However, the available 11-month GNIP-dataset (IAEA/WMO, 2018) has been mainly applied for their interpretation that prevented a full quantitative interpretation of the regional isotope records (Swann et al., 2018). Consequently, a comprehensive reference dataset on the isotopic composition of atmospheric precipitation would contribute to a number of regional projects dealing with the past, present and future climate development.

To fill the current knowledge gap, this article presents a new dataset of 284 precipitation samples collected between June 2011 and October 2013 and from December 2014 to April 2017 in Irkutsk, a representative site for the Baikal region in southeast Siberia. The specific objectives of the study are to (a) examine the seasonality of isotope signals in precipitation, (b) reveal which of the meteorological

variables control the precipitation isotope signal, (c) assess the ability of climate model simulated stable isotopes to capture variations in the measured data, and (d) investigate backward trajectories generated by the Hybrid Single-Particle Lagrangian Integrated Trajectory (HYSPLIT) model and to infer the influences of different moisture sources on stable isotope variations in precipitation. The isotope data of Irkutsk precipitation in combination with the modelled and meteorological data and reconstructed dominant air-mass pathways and moisture source regions may lead to a better understanding of the response of precipitation stable isotope composition to climatic changes and, thus, improve the background information for climate reconstructions both in the Baikal region in particular and in continental Eurasia in general.

2 | STUDY AREA

Southeastern Siberia with Lake Baikal (Figure 1) is located in the centre of the Eurasian continent, far from oceanic influences. Irkutsk (52°18′N, 104°17′E; 469 m asl; Figure 1) is the regional centre and the largest city with a population of half a million. The climate conditions of Irkutsk are typical for the whole region. The area is known for its extreme continental climate expressed in large seasonal variations of air temperatures, with daily mean values ranging from −50°C in January to +37°C in July (Lydolph, 1977; Shver & Formanchuk, 1981). Figure 2 shows mean monthly temperatures and precipitation sums for the city of Irkutsk. The mean annual air temperature of +0.0 ±1.3°C and the mean annual precipitation sum of 429±97 mm were recorded for the period 1887–2014. This indicates a cold, snow-dominated environment with negative temperatures for 6 months of the year (October to March).

The Atlantic westerlies and the Siberian high are dominant synoptic phenomena, determining regional atmospheric circulation and climate (Gustokashina, 2003; Ladeischikov, 1977; Lydolph, 1977; Shver & Formanchuk, 1981). Precipitation throughout the year is mainly associated with cyclones of western or northwestern origin. Although in July and August, when the high-pressure centre is located in Yakutia, southerly cyclones from Mongolia enter the region, bringing warm and relatively humid air, often causing heavy rainstorms. Intrusions of cold Arctic air from the Kara Sea during autumn cause widespread cooling and initiate the development of the Siberian high. The high-pressure cell, cantered on southeastern Siberia and Mongolia, lasts until the following April. Precipitation is usually low during this period

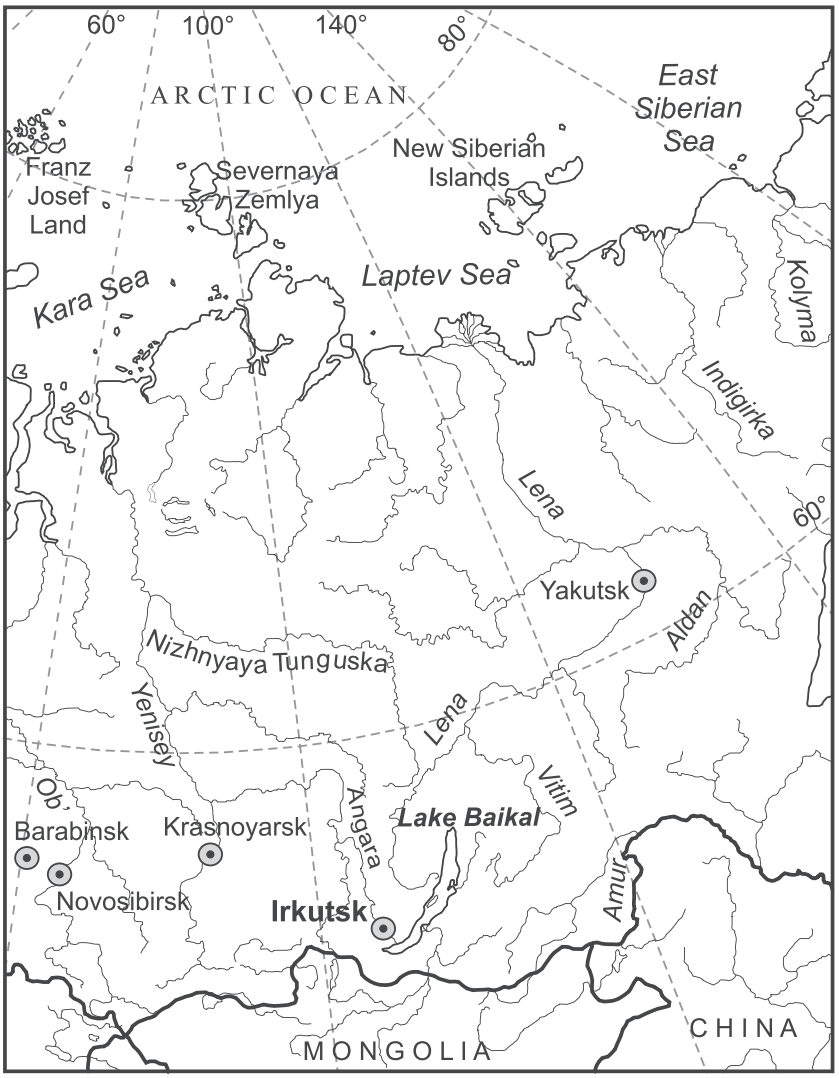

FIGURE 1 Schematic map of Eastern Siberia including the study site, the city of Irkutsk, situated close to Lake Baikal, and other points of interest

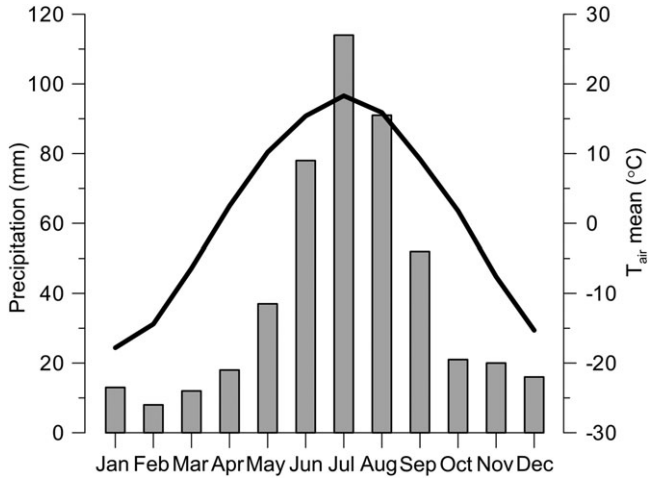

FIGURE 2 Summary climate data for the city of Irkutsk: average monthly precipitation amount (grey rectangle) and average monthly air temperature (black line) based on meteorological data provided by the National Oceanic and Atmospheric Administration and the National Climatic Data Center (available at: www.ncdc.noaa.gov/data-access/quick-links)

(Figure 2) and the cold and sunny weather prevails in the region (e.g., Lydolph, 1977; Shver & Formanchuk, 1981).

3 | MATERIALS AND METHODS

Event-based (or daily) stable water isotope data can be linked to the dynamics of atmospheric moisture more directly than monthly data and thus allow for a better understanding of the origin and trajectories of the air masses (e.g., Sánchez-Murillo, Durán-Quesada, Birkel, Esquivel-Hernández, & Boll, 2017). In total, 284 event-based precipitation samples were collected in Irkutsk during the time period from June 2011 to October 2013 and from December 2014 to April 2017. We used a polyethylene container and a funnel attached to a column ~5 m above ground level (agl) to avoid contamination, for example, by windblown snow from previous events. Samples were collected from the container at the end of each precipitation event to minimize evaporation and sublimation effects. Rainwater was directly placed into airtight bottles, and snow samples were first thawed at room temperature. All samples were stored cool until isotope analysis. During the considered periods, the monitoring of precipitation covers every month of the year at least three times.

All hydrogen and oxygen isotope measurements were performed at the Isotope Laboratory of the Alfred Wegener Institute Helmholtz Centre for Polar and Marine Research (AWI Potsdam, Germany) with a Finnigan MAT Delta-S mass spectrometer equipped with equilibration units following a procedure described in Meyer, Schönicke, Wand, Hubberten, and Friedrichsen (2000). The $\delta^{18}O$ and δD values are given as permil difference to Vienna Standard Mean Ocean Water (‰, VSMOW). The accuracy of this method is better than ±0.8‰ and ±0.1‰ for δD and $\delta^{18}O$, respectively (Meyer et al., 2000).

To characterize the recent local moisture conditions, different basic parameters were calculated from the measured isotope data. The mean monthly (δ_{mm}) and weighted mean monthly (δ_{wm}) isotopic compositions of precipitation were computed applying the equations of Yurtsever and Gat (1981):

$$\delta_{mm} = \frac{\sum \delta_i}{\sum i}, \quad (1)$$

$$\delta_{wm} = \frac{\sum (P_i \times \delta_i)}{\sum P_i}, \quad (2)$$

where δ_i denotes the isotopic composition of a precipitation event (‰), i denotes the total number of precipitation samples, and P_i denotes the precipitation amount (mm). Furthermore, 2011–2017 averages of monthly means were calculated for $\delta^{18}O$, δD, and d excess wherever more than one datapoint for a discrete month was available. Local meteoric water lines (LMWL) were derived from the correlation between $\delta^{18}O$ and δD and compared with the global meteoric water line (GMWL; $\delta D = 8 \times \delta^{18}O + 10$; Craig, 1961). The deuterium excess (d excess = $\delta D - 8 \times \delta^{18}O$) introduced by Dansgaard (1964) as an indicator for nonequilibrium fractionation processes is generally related to conditions (i.e., humidity and sea surface temperature) of the initial moisture source region and commonly invariable during condensation of vapour masses (Merlivat & Jouzel, 1979). However, the d excess may also be indicative for secondary fractionation processes such as the participation of recycled moisture, that is, from open water bodies situated between the primary moisture source and the region of precipitation (Gat, 2000; Kurita et al., 2003, 2005).

During condensation and precipitation of moisture, a depletion of $\delta^{18}O$ and δD is due to temperature-dependent isotope fractionation and follows a Rayleigh distillation process (Merlivat & Jouzel, 1979). Consequently, the evolution of $\delta^{18}O$ and δD is directly related to air temperatures and to the distance from the moisture source. Hence, the obtained isotope data are compared with major regional meteorological and synoptic features. For this purpose, meteorological data (temperature, dew point, and precipitation amount) for Irkutsk (Station ID: 30710099999) were derived at daily resolution from the global summary of the day datasets provided by the National Oceanic and Atmospheric Administration (NOAA) and the National Climatic Data Center (NCDC; available at: www.ncdc.noaa.gov/data-access/quick-links) converted into metric units. Relative humidity (rH) at the studying site was calculated from temperature and dew point:

$$rH = \frac{E_{Sd}}{E_{St}}, \quad (3)$$

where E_{sd} and E_{st} denote the saturation vapour pressure of dew point and temperature, respectively (Alduchov & Eskridge, 1996; Lowe & Ficke, 1974):

$$E_s = 6.107 \times 10^{\frac{7.5 \times t}{(t+273.3)}}, \text{over water surface } (t_d, t > 0), \quad (4)$$

$$E_s = 6.107 \times 10^{\frac{9.5 \times t}{(t+265.5)}}, \text{over ice surface } (t_d, t < 0), \quad (5)$$

where t_d and t denote dew point and temperature in °C.

Measured daily isotope values are compared against modelled values retrieved from an European Centre/Hamburg version 5 (ECHAM5)-wiso simulation. ECHAM5-wiso (Werner et al., 2011) is the isotope-enabled version of the ECHAM5 atmosphere global climate model (Roeckner et al., 2006). The water cycle in ECHAM5 contains formulations for evapotranspiration of terrestrial water, evaporation of ocean water, and the formation of large-scale and convective clouds. The stable water isotope module in ECHAM5 computes the isotopic signal of different water masses through the entire water cycle, including that in precipitation and soil water. Model values for Irkutsk were retrieved from an ECHAM5-wiso simulation using an implicit nudging technique (Butzin et al., 2014) to constrain simulated fields of surface pressure, temperature, divergence, and vorticity to the corresponding ERA-40 and ERA-Interim reanalysis fields (Dee et al., 2011). The considered simulation period is between June 2011 and April 2017, and the horizontal grid resolution was 1.1° × 1.1° (T106 spectral truncation). Days with modelled precipitation of less than 0.5 mm were excluded from isotope statistics as this is also the threshold for sampled precipitation.

To identify the probable moisture provenance, 5-day air-parcel backward trajectories were calculated for every single precipitation event registered in Irkutsk using the HYSPLIT model (Draxler & Hess, 1998; Stein et al., 2015). We focused on the trajectories arriving at 2,000 m agl (around pressure level of 850 hPa) as most of tropospheric moisture is contained up to 2,000 m agl, and at the same time to avoid any low-altitude topographical interferences (e.g., Krklec & Domínguez-Villar, 2014). The model calculates a three-dimensional displacement of air parcels using gridded meteorological data. The Global Data Assimilation System (GDAS1) archive, which runs globally every 6 hr with 1° latitude and longitude resolution (http://ready.arl.noaa.gov/gdas1.php) has been applied. Later on, single trajectories were grouped in four major groups or clusters for the studied station, following a statistical treatment that calculates the total spatial variance (TSV) of the trajectories beginning with as many clusters (N_c) as trajectories (N_t). In an iterative process the trajectories are combined to produce $N_c = N_t - 1$, $N_t - 2$, until $N_c = 1$. The clusters combined are those with the least TSV difference at each step. The final number of clusters is chosen when the clusters being grouped show a great increase in their TSV (clusters grouped are not anymore similar). The HYSPLIT model and more detailed information of its statistical background are freely available from the NOAA's Air Resource Laboratory website (Draxler & Rolph, 2015).

4 | RESULTS

4.1 | 4.1. Variations in δ and *d* excess values

Stable isotope data for all individual precipitation events (i.e., all collected rain and snow samples) in the city of Irkutsk during the study period are summarized in Table 1 and presented in a $\delta^{18}O$–δD diagram

TABLE 1 Summary of Stable Isotope Composition ($\delta^{18}O$, δD, and *d* Excess), Which Includes Minimum, Mean and Maximum Values, Standard Deviations (*SD*), Slopes, Intercepts, Coefficient of Determination (r^2), and Significance Level (*p*) From the $\delta^{18}O$–δD Diagram for Irkutsk Precipitation Events

Sample type	n	$\delta^{18}O$ (‰) min	$\delta^{18}O$ (‰) mean	$\delta^{18}O$ (‰) max	$\delta^{18}O$ (‰) *SD*	δD (‰) min	δD (‰) mean	δD (‰) max	δD (‰) *SD*	*d* excess (‰) min	*d* excess (‰) mean	*d* excess (‰) max	*d* excess (‰) *SD*	Slope	Intercept	r^2	*p*
Rain	137	−24.8	−11.7	−4.4	4.0	−189.1	−92.6	−39.6	29.4	−19.0	1.0	15.1	8.4	7.1	−10.2	0.93	<.01
Snow	147	−41.4	−26.7	−12.0	6.1	−322.4	−205.3	−79.6	50.0	−17.4	9.0	33.3	8.1	8.1	10.9	0.97	<.01

(Figure 3a) with reference to the GMWL, in which precipitation is correlated on global scale (Rozanski et al., 1993). Mean monthly isotope data during the study intervals between June 2011 and April 2017 and meteorological parameters are given in Table S1. The stable isotope composition of event-based precipitation varies in wide range of −41.4 and −4.4‰ for $\delta^{18}O$ and of −322.4 and −39.6‰ for δD. Rain samples (n=137) are characterized by relatively higher mean $\delta^{18}O$ and δD values of −11.7‰ and −92.6‰, respectively, and lower d excess = +1.0‰ whereas snow samples (n=147) display relatively lower mean $\delta^{18}O$ = −26.7‰ and δD = −205.3‰ and higher d excess of +9.0‰.

For the period between June 2011 and April 2017, the Irkutsk stable isotope composition yield respective mean single event-based (n = 284), weighted monthly means (n = 55), and weighted mean annual (n = 12) values of −19.4‰, −19.7‰, and −19.5‰ for $\delta^{18}O$, corresponding −150.8‰, −151.6‰, and −150.4‰ for δD and +5.1‰, +6.1‰, and +6.1‰ for d excess. Data of the averages of weighted mean monthly for the considered time interval are presented in Table 2.

Weighted mean annual precipitation $\delta^{18}O$ = −19.5‰ and δD = −150.4‰ are significantly lower than the GNIP data: $\delta^{18}O$ = −16.2‰, δD = −124.1‰ (IAEA/WMO, 2018). This is probably due to (a) missing values in GNIP for December and (b) the considered time intervals (11 months of a single year [GNIP database] versus 55 months of a close to 5-year interval). However, both mean annual d excess values (+5.3‰ GNIP database and +6.2‰ our data) are similar indicating constant general synoptic patterns captured by the two datasets.

4.2 | 4.2. Local meteoric water lines

The LMWL based on all single events (Figure 3a) was determined as the relationship $\delta D = 7.6 \times \delta^{18}O - 3.3$ (r^2 = 0.98; p <.01; n = 284). This line is in a good agreement with the LMWL from weighted monthly means with a slope of 7.7 and an intercept of +0.7 (r^2 = 0.99; p <.01; n = 55) and also from weighted mean annual with a slope of 7.8 and an intercept of +1.2 (r^2 = 0.99; p <.01; n = 12). Minor differences between the LMWLs based on single events and weighted mean data mainly result from calculations of precipitation amount and averaging effects. All obtained LMWLs have smaller slopes and intercepts compared with the GMWL, and they are slightly shifted below the GMWL, mainly due to the rainwater samples with lower average d excess values compared with the global d excess of +10‰ (Figure 3a).

To analyse differences between the isotopic composition of snow and rain, the LMWL was subdivided into LMWL-rain and LMWL-snow (Table 1 and Figure 3a). The LMWL-snow has a similar slope to the GMWL (8.1) and an intercept of +10.9‰ (Table 1). In contrast, the isotope composition of rain differs strongly from the GMWL as displayed by a lower slope of 7.1 and intercept of −10.2‰. Compared with event-based rain samples with d excess varying between −19.0‰ and +15.1‰, snow has a higher range in d excess from −17.4‰ to +33.3‰.

4.3 | 4.3. Isotope-temperature dependence

A linear relationship between isotope ratio single precipitation events and daily mean temperatures has been calculated (n=284): $\delta^{18}O = 0.62 \times T_{air} - 19.6$ (r^2 = 0.79; p <.01) and $\delta D = 4.6 \times T_{air} - 152.3$ (r^2 = 0.77; p <.01). If weighted mean monthly precipitation (n = 55) and monthly temperatures (including days only with precipitation) are used, $\delta^{18}O/T$ and δD/T coefficients become slightly lower, as +0.57‰/°C (r^2 = 0.87; p <.01) and +4.4‰/°C (r^2 = 0.87; p <.01), respectively. $\delta^{18}O$–T and δD–T relationships for weighted mean monthly precipitation and mean monthly temperatures (n = 55; Figure 4a and Table 3) are also characterized by lower coefficients of +0.50‰/°C (r^2 = 0.85; p <.01) for $\delta^{18}O$ and +3.9‰/°C (r^2 = 0.85; p

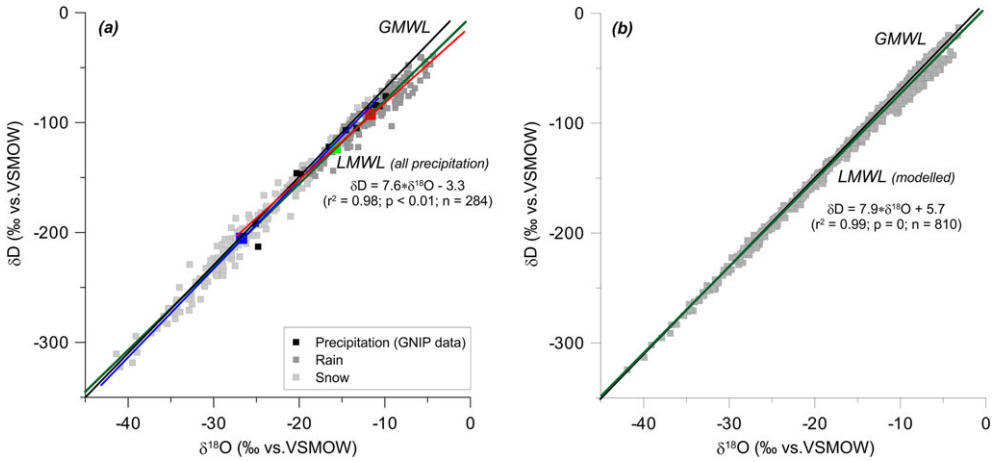

FIGURE 3 The correlation between precipitation δD and $\delta^{18}O$ in Irkutsk from June 2011 to April 2017: (a) collected event-based samples. Arithmetic mean snow (blue square) and rain (red square) values are displayed. Global meteoric water line (black) defined by Craig (1961). Local meteoric water line (LMWL; green) subdivided into LMWL-snow (blue) and LMWL-rain (red) derived from local precipitation isotope data (own data; Table 1). Additionally, Global Network for Isotopes in Precipitation data (means for 11 months, Irkutsk) and Lake Baikal mean isotope composition (light-green square) are given; (b) daily data simulated by the European Centre/Hamburg version 5 (ECHAM5)-wiso climate model

TABLE 2 The Averages of Weighted Mean Monthly $\delta^{18}O$, δD, and *d* Excess for Irkutsk Precipitation Between June 2011 and April 2017

	Measured data				Modelled by ECHAM5-wiso data			
Month	*n*	$\delta^{18}O$ (‰)	δD (‰)	*d* excess (‰)	*n*	$\delta^{18}O$ (‰)	δD (‰)	*d* excess (‰)
January	5	−30.0±2.3	−232.1±21.8	8.6±3.8	6	−25.5±1.0	−196.7±8.4	7.7±0.5
February	5	−27.0±2.1	−214.8±21.4	1.9±7.0	6	−26.8±3.2	−207.4±26.9	6.9±2.5
March	4	−21.8±3.4	−168.6±31.5	6.1±5.8	6	−17.8±2.0	−134.8±15.7	7.8±0.8
April	4	−15.3±3.9	−113.3±27.9	9.1±7.8	6	−13.1±1.4	−95.7±11.6	9.0±0.9
May	3	−13.3±2.9	−104.0±19.8	2.4±4.2	5	−12.8±1.3	−93.4±10.8	8.7±0.8
June	5	−12.7±1.7	−102.7±7.4	−0.7±6.0	6	−10.5±0.9	−76.9±8.1	6.7±1.4
July	5	−11.0±1.5	−84.6±17.7	2.7±5.1	6	−9.0±1.3	−64.9±10.8	6.8±1.0
August	5	−12.1±1.3	−90.0±6.6	6.0±4.8	6	−10.0±1.8	−72.0±16.0	8.4±1.6
September	5	−14.9±1.2	−113.9±8.4	5.5±5.9	6	−13.0±2.7	−92.8±22.6	10.9±2.2
October	5	−22.4±6.1	−166.9±46.1	11.8±3.8	6	−19.5±3.4	−145.7±27.1	10.2±1.2
November	4	−25.4±4.2	−192.6±29.2	10.3±6.8	6	−23.4±4.7	−177.0±37.7	10.1±0.8
December	5	−28.8±3.8	−221.0±26.2	9.1±5.8	6	−24.7±3.7	−188.8±29.7	8.8±1.4

<.01) for δD due to the fact that during the winter, the air temperatures on precipitation days are higher than on days without precipitation and opposite in the summer.

A negative (−0.13‰/°C; Table 3) and statistically not significant (r^2 = 0.08; p =.03) correlation was found between weighted mean monthly *d* excess and temperature (Figure 4b), mainly due to the dependence of *d* excess on evaporation and the lack of further modifications during the rain-out process (Merlivat & Jouzel, 1979). For Irkutsk, this correlation is, however, enhanced by the addition of recycled moisture with low *d* excess in summer (Table 2).

4.4 | 4.4. Comparison of measured and modelled stable isotope data

Discrete isotopic measurements and atmospheric observations were simulated by the ECHAM5-wiso model for the complete observation period from June 2011 to April 2017 (Figures 5 and 6 and Tables 2 and S2). Modelled data refer to a grid box of 1° × 1°, whereas measured samples derive from one discrete sampling station. Nonetheless, measured and modelled datasets correspond in general quite well despite some obvious notable differences. The modelled LMWL has a generally similar slope to the GMWL of 7.9 and slightly lower intercept of +5.7‰ (Figure 3b). Differences between the LMWL-measured (Figure 3a) and LMWL-modelled could indicate that ECHAM5-wiso does not fully capture secondary evaporation effects during the summer months. Comparing modelled and measured mean monthly data yield an excellent agreement for temperature (r^2 = 0.99; p <.01; n = 71), precipitation amount (r^2 = 0.72; p <.01; n = 71), and weighted $\delta^{18}O$ (r^2 = 0.87; p <.01; n = 55), whereas weighted *d* excess displays a very low correlation (r^2 =.14; p <.01; n = 55). Both modelled $\delta^{18}O$ and temperatures display distinct seasonal cycling, although they show a lower variability compared with the measured data (Figure 6). Additionally, ECHAM5-wiso seems to slightly overestimate the absolute $\delta^{18}O$ values (Figure 6a and Table 3) and underestimate temperatures especially for the first half of the year (Figure 6c). Modelled *d* excess (Figure 6b) displays an unclear seasonal cycle and a much lower variability contrasting with the measured data. The reason for this difference is unclear and can partly explained by the observation that ECHAM5-wiso simulation does not seem to capture well the processes associated with secondary moisture supply in summer.

Moreover, there is strong agreement between our measured mean monthly isotope values and Online Isotopes in Precipitation Calculator (OIPC)-modelled values (Online Isotopes in Precipitation Calculator; Bowen, 2019) for Irkutsk (r^2 = 0.86; p <.01; n = 12). However, the OIPC underestimates $\delta^{18}O$ on the annual scale (a mean annual value of −12.6‰ vs. measured −19.4‰). This discrepancy probably reflects the inability of the model to capture local-scale processes such as secondary evaporation effects and/or seasonal shifts in air mass trajectories. Additionally, because the density of observations in the investigated region is low, these differences may be due to the spatial interpolation method applied by Bowen (2019).

5 | DISCUSSION

5.1 | 5.1. Seasonal variations in isotope data

Stable isotope data for Irkutsk precipitation show distinct seasonal variations (Figure 5). Rainwater samples are characterized by relatively high $\delta^{18}O$ and δD values of up to −4‰ and −40‰, respectively (Table 1), and snow samples generally show lighter isotopic composition, which may drop to $\delta^{18}O$ = −41‰ and δD = −322‰. Rain samples mainly plot in the upper right part of the $\delta^{18}O$–δD diagram below the GMWL (Figure 3a) indicating the participation of secondary fractionation processes, that is, due to recycled moisture (Kurita et al., 2003, 2004; Numaguti, 1999). Previous studies (Koster, de Valpine, & Jouzel, 1993; Numaguti, 1999; Ueta et al., 2013; Ueta, Sugimoto,

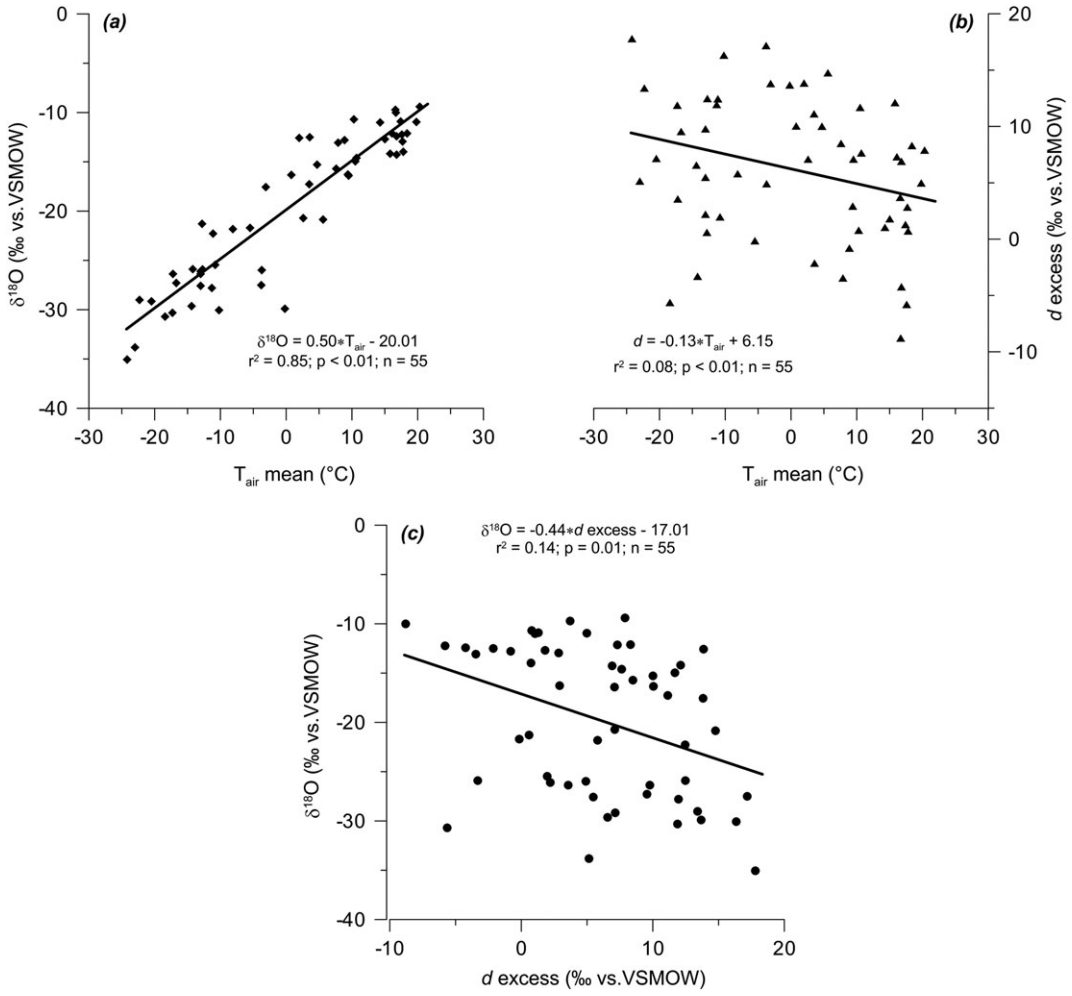

FIGURE 4 Correlations between (a) weighted mean monthly precipitation $\delta^{18}O$, (b) weighted mean monthly *d* excess and mean monthly temperature, (c) weighted mean monthly precipitation $\delta^{18}O$, and weighted mean monthly *d* excess

TABLE 3 Correlation Between Weighted Mean Monthly Isotopic ($\delta^{18}O$, δD, and *d* Excess) and Mean Monthly Meteorological (rH, P, and T) Parameters of Irkutsk

		P (mm)			rH (%)			T_{air} (°C)		
Correlation parameter	***n***	**Slope**	r^2	***p***	**Slope**	r^2	***P***	**Slope**	r^2	***p***
$\delta^{18}O$ (‰)	55	0.10	0.26	<.01	−0.27	0.16	<.01	0.50	0.85	<.01
δD (‰)	55	0.78	0.27	<.01	−2.07	0.15	<.01	3.91	0.85	<.01
d excess (‰)	55	−0.02	0.01	.46	0.12	0.04	.13	−0.13	0.08	.03

Abbreviation: rH, relative humidity.

Iijima, Yabuki, & Maximov, 2014) have demonstrated that evapotranspiration significantly contributes to rain and the moisture recycling rate in eastern Siberia can exceed 85% during summer months (Risi, Noone, Frankenberg, & Worden, 2013). A large area occupied by high number of lakes, rivers, and mires in western Siberia may act as secondary moisture sources for summer precipitation in eastern Siberia (Koster et al., 1986; Kurita et al., 2003). Secondary evaporation from open water bodies tends to enrich the rainwater in the heavy isotopes with a tendency to lower *d* excess (Stewart, 1975). Our results indicate that Irkutsk rain receives admixed water vapour from a secondary moisture source enriched in heavy ^{18}O and ^{2}H isotopes and characterized by lower *d* excess as compared with snow.

At the same time, snow samples display a much lighter isotopic composition and are located close to the GMWL (Figure 3a) suggesting an origin from the initial moisture source. Snow precipitation is characterized by relatively high *d* excess values as compared with rain (Table 1) due to nonequilibrium condensation during the growth of the snow particles (Gat, 2000; Jouzel & Merlivat, 1984).

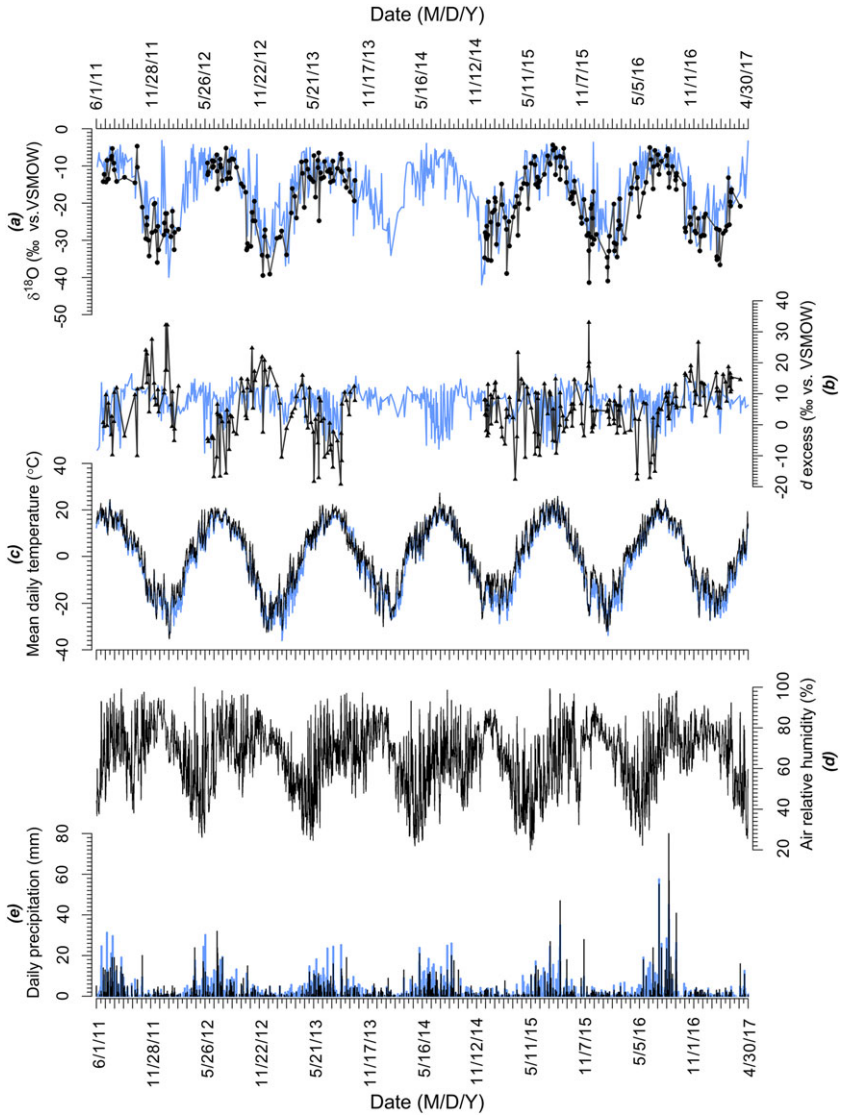

FIGURE 5 Time series of (a) precipitation $\delta^{18}O$ values and (b) *d* excess (own data), (c) mean daily temperature and (e) daily amount of precipitation derived from the global summary of the day datasets (available at: www.ncdc.noaa.gov/data-access/quick-links), and (d) air relative humidity in the study area. Both measured/observed data (black) and data simulated by the European Centre/Hamburg version 5 (ECHAM5)-wiso climate model (blue) are displayed

High values of *d* excess may be associated with intense oceanic evaporation during winter (Pfahl & Sodemann, 2014). The large humidity gradients over the ocean surface lead to strong nonequilibrium fractionation resulting in high *d* excess values. Moreover, the isotopic signal of snow in Irkutsk could be affected by evaporated water from Lake Baikal (mean $\delta^{18}O_{lake}$ = −15.8 ± 0.2‰, Seal & Shanks, 1998; Figure 3a) as a secondary moisture source, from which evaporation tends to be active during the late autumn and early winter (November/December; Shimaraev, Verbolov, Granin, & Sherstyankin, 1994). However, due to predominance of the westerly circulation, the lake effect to Irkutsk snow seems to be negligible.

The weighted mean monthly isotope composition of Irkutsk precipitation (Figure 6a) exhibit a clear annual cycle closely following the seasonal temperatures (Figure 6c). Weighted mean monthly $\delta^{18}O$ values (Figure 6a) have a higher variability during March–April and in October–November when precipitation in the region can fall both as rain and as snow. Unlike weighted mean monthly $\delta^{18}O$ values, weighted mean monthly *d* excess values exhibit two maximum peaks close to or slightly higher than 10‰ in October–November and in April (Figure 6b) showing conditions of evaporation at moisture source close to the global average (Rozanski et al., 1993). February and May–July are characterized by rather low *d* excess values <5‰ probably displaying higher humidity conditions in moisture sources (Gat, 2000) and/or contribution of continental recycled moisture. Low *d* excess values in May–July could also be associated to secondary evaporation during rainfall (Clark & Fritz, 1997; Gat, Mook, & Meijer, 2001).

The weighted mean monthly $\delta^{18}O$ and δD values of winter (December–February) and summer (June–August) precipitation in Irkutsk are = −28.6‰ and −11.9‰, = −222.6‰ and −92.4‰, as well as *d* excess = +6.5‰ and +2.7‰, respectively. Our weighted mean monthly summer precipitation values are similar to those of the GNIP database (IAEA/WMO, 2018) with −11.4‰ for $\delta^{18}O$ and −88.1‰ for δD, +3.2‰ for *d* excess, and winter values (GNIP: $\delta^{18}O$ = −25.0‰, δD = −202.5‰, and *d* excess = −2.9‰) all differ significantly from

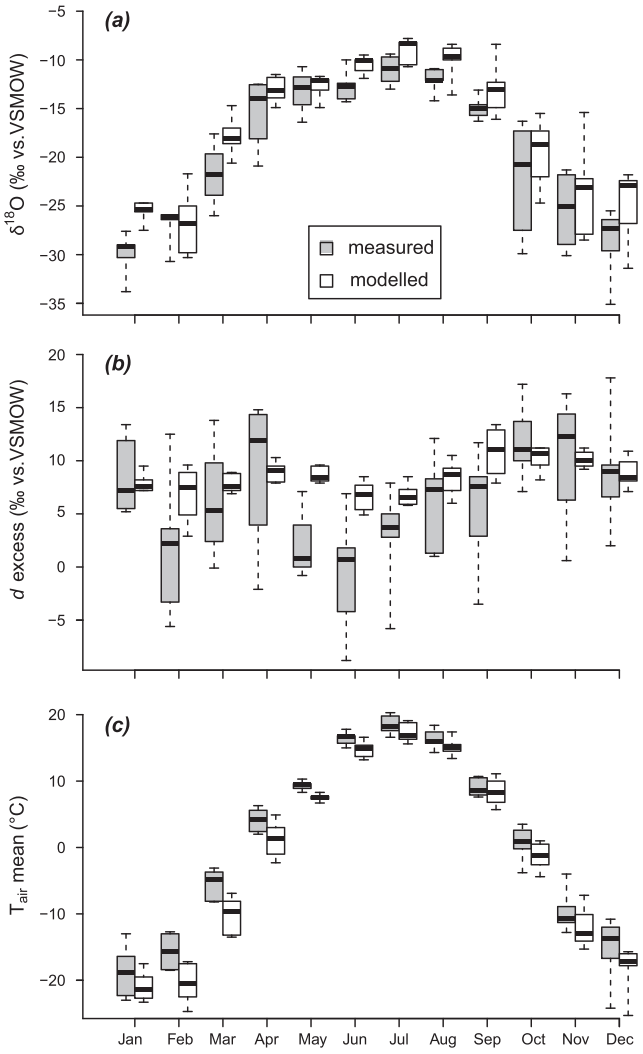

FIGURE 6 The annual variations of (a) weighted mean monthly precipitation $\delta^{18}O$, (b) weighted mean monthly *d* excess and (c) mean monthly temperature for period from June 2011 to April 2017. The box-and-whisker plots present the median (black bar), the 0.25 and 0.75 quartiles (grey box edges), and the minimum and maximum values (whiskers)

our calculations probably due to missing data for December in the GNIP dataset, as mentioned above.

Generally, Irkutsk weighted mean monthly $\delta^{18}O$ and δD values for winter and summer are higher than those obtained for Yakutsk (−33.0‰ and −12.9‰ for $\delta^{18}O$, −265.8‰ and −106.0‰ for δD; Kurita et al., 2004; Papina et al., 2017) located 1,900 km northeast of Irkutsk (Figure 1), but lower than those for Barabinsk (−20.2‰ and −8.0‰ for $\delta^{18}O$, −155.7‰ and −65.3‰ for δD; Kurita et al., 2004) situated 1,700 km west of Irkutsk. This is presumably due to a notable continental effect caused by gradual rainout when air masses move over the continent, a process generally accompanied by isotope depletion (Araguás-Araguás et al., 2000; Kurita et al., 2004; Rozanski et al., 1993). The weighted mean monthly winter *d* excess in Irkutsk with +6.5‰ is significantly higher than that for Yakutsk (−1.8‰; Kurita et al., 2004) and comparable to Barabinsk (+5.9‰) and summer *d* excess in Irkutsk (+2.7‰) is higher than that for Yakutsk (−2.8‰) and for Barabinsk (−1.3‰). The differences in *d* excess between Irkutsk and Yakutsk/Barabinsk are probably caused by differences of synoptic patterns or moisture sources for both sites (Kurita, 2011; Kurita et al., 2005; Latysheva, Sinyukovich, & Chumakova, 2009; Papina et al., 2017). Additionally, differences in isotopic parameters could also partly be related to differences in mean annual air temperature (−7.0°C for Yakutsk and +2.1°C for Barabinsk; Kurita et al., 2005) and mean annual precipitation amount (230 mm for Yakutsk and 371 mm for Barabinsk; Kurita et al., 2005).

5.2 | 5.2. Implications of the isotope-temperature dependence for palaeoclimate interpretation

Temperature is one of the main controls for water isotope composition in precipitation (Craig, 1961; Dansgaard, 1964). For palaeoclimate reconstruction, the correlation between $\delta^{18}O$ (δD) and air temperatures is essential, and especially significant for continental regions, as southeastern Siberia, where annual temperature amplitudes are largest. Whereas marine sites often display low annual $\delta^{18}O/T$ gradients of 0.15 to 0.25 ‰/°C (e.g., Clark & Fritz, 1997), continental sites are characterized by a much higher average $\delta^{18}O/T$ coefficient of 0.58‰/°C (Clark & Fritz, 1997; Rozanski et al., 1993). However, site-specific $\delta^{18}O/T$ relationships may vary on different timescales (as observed in ice cores, e.g., Casado et al., 2017).

The low $\delta^{18}O/T$ coefficient of 0.36‰/°C between mean monthly temperatures and weighted mean monthly precipitation $\delta^{18}O$ was suggested for the Lake Baikal region (Seal & Shanks, 1998). It was used to interpret palaeoclimatic records (e.g., oxygen isotopes in biogenic silica) from lakes of the Baikal region (Kostrova et al., 2013; Mackay et al., 2011; Morley et al., 2005), and consequently yielded a rather low influence of air temperature on changes in regional proxy-based isotope records. Kostrova et al. (2014) suggested a distinctly higher $\delta^{18}O/T$ gradient of 0.57‰/°C for Irkutsk single precipitation events, which was interpreted as a change in precipitation $\delta^{18}O/T$ patterns. Both gradients were derived from a very limited amount of data.

Using the current dataset, we suggest that the $\delta^{18}O/T$ gradient of 0.50‰/°C is more reliable and should be used in future studies. In addition, (a) this value resembles a typical gradient value reported for other continental regions of Siberia, that is, central Yakutia (Papina et al., 2017); (b) it is based on a full year of data (in contrast to coefficient of 0.36‰/°C based on 14 single data points covering only 11 months) and, hence, more representative. The $\delta^{18}O/T$ gradients in the city of Irkutsk, calculated for single years from 2011 to 2017, vary between 0.44 and 0.54‰/°C, never being as low as it was suggested by Seal and Shanks (1998). This conclusion is one of the highlights of the current study and underlines our assumption that for the study region, higher than previously assumed $\delta^{18}O/T$ gradient is likely to increase the significance of air temperature for the isotope-based proxy records and for the palaeoclimatic reconstructions.

5.3 | Correlation with other meteorological parameters

As $\delta^{18}O$ and δD values are highly correlated, the following results are given for $\delta^{18}O$ only. A negative correlation was observed between $\delta^{18}O$ and *d* excess (Figure 4c) with relatively higher summer $\delta^{18}O$ generally coinciding with lower *d* excess (Figure 5) probably due to the seasonal character of moisture supply by predominant north-westerly transport in winter (Kurita et al., 2004), as well as westerlies/south-westerlies in summer, with additional contribution of recycled moisture (Koster et al., 1986; Kurita, 2011; Numaguti, 1999).

To evaluate the influence of rH and precipitation amount (P) on the isotope signal, correlations between weighted mean monthly isotope data and other meteorological parameters were determined. A positive correlation was specified between $\delta^{18}O$ and P, whereas that with *d* excess is negative (Table 3). A negative correlation was also identified between $\delta^{18}O$ (δD) and rH, and *d* excess correlates positively with rH. All these dependencies are characterized by low correlation coefficients r^2 varying from 0.01 to 0.27 (Table 3). Therefore, we conclude that neither rH nor P have strong impact on the isotope signal of precipitation in Irkutsk. Air temperature is the first-order control and explains ~85% of variability in δ-values.

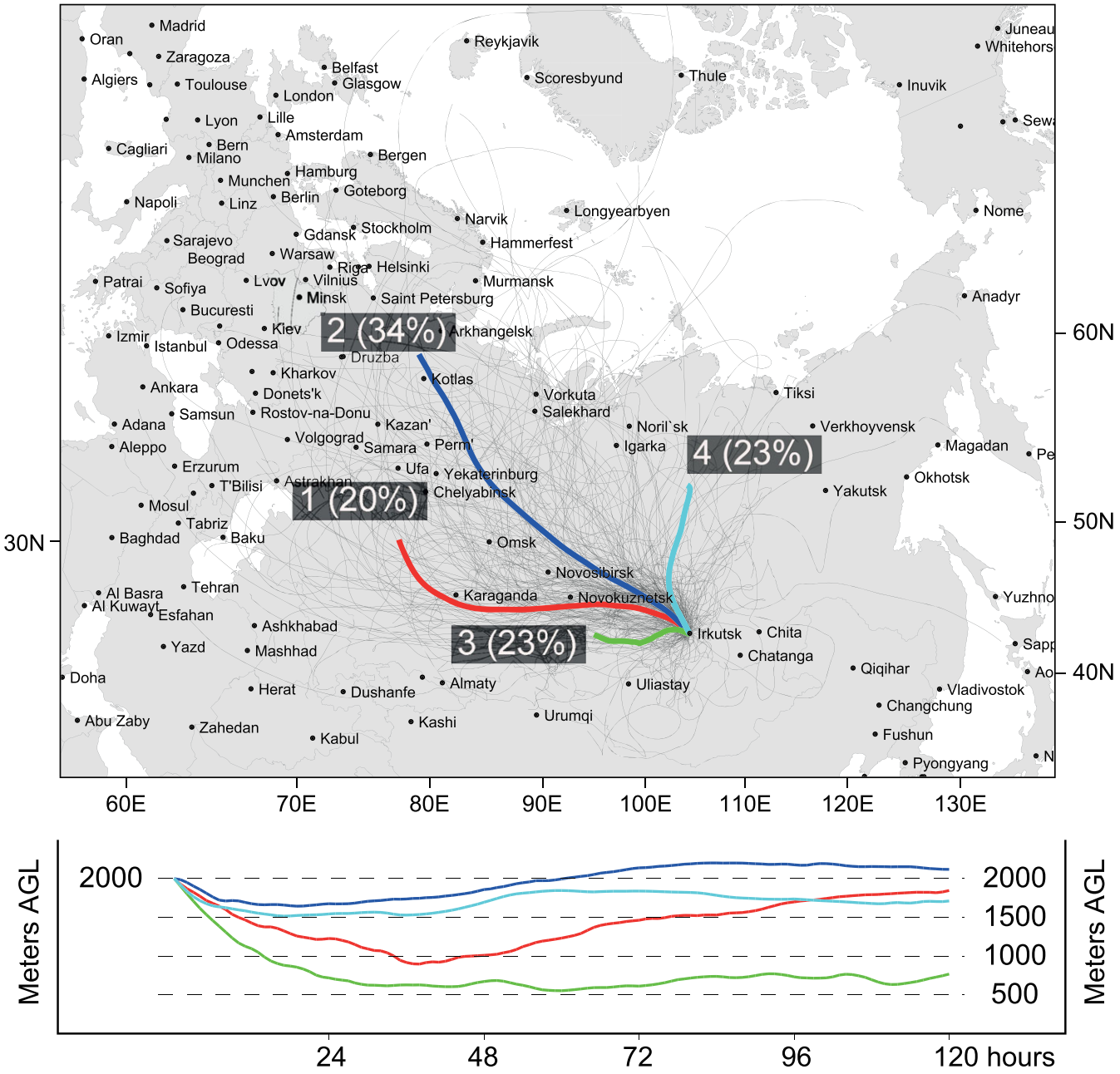

FIGURE 7 Backward trajectories analysis (5-day, 120 hr) for a total of 284 single trajectories calculated at pressure level of 850 hPa for all registered single precipitation events between June 2011 and April 2017. Four main backward trajectory clusters for all precipitation events reaching Irkutsk including their vertical profile

5.4 | 5.4. Relationship between variations of isotope composition and moisture source

Variations in the isotope composition of precipitation are defined not only by local condensation temperatures (Dansgaard, 1964) but also by the origin and history of air-mass trajectories (Kurita, 2011). The trajectory—as the path of an air mass before reaching a given sampling site—receives a characteristic isotopic signature dependent on the meteorological conditions in the moisture source region (Merlivat & Jouzel, 1979). Therefore, it is possible to differentiate between potential primary sources and the influence of secondary moisture of open water bodies that are located on the track of an air mass. Reconstruction of 5-day backward circulation paths of every single precipitation event registered in Irkutsk during the studied period is shown in Figure 7. This figure presents a wide distribution of the trajectories varying in their origin from the Arctic Ocean in the north to the northern China and Mongolia regions in the south. The easterly transport occurs rarely; that is, only four cases are registered for the monitoring period. Most of the trajectories originate from the west and follow a general pattern observed in eastern Siberia, in line with many regional atmospheric studies (Gustokashina, 2003; Ladeischikov, 1977; Latysheva et al., 2009; Loshchenko, 2015; Marchenko, Mordvinov, & Berezhnykh, 2012; Osipova & Osipov, 2016).

To identify the regions, from where the precipitation events preferentially might have originated, all reconstructed trajectories were combined into four main clusters (Figure 7) until minimal differences between trajectories within a cluster and maximal differences between clusters were reached and a further decrease in the number of clusters led to a significant increase in TSV (Draxler & Rolph, 2015).

The dominant direction of air masses arriving at Irkutsk clearly originates from the west (clusters 1–3) including parts of Europe, western part of Russia, and northern Kazakhstan, with about 77% of all precipitation events in the Baikal region. About 23% of precipitation events indicate moisture pathways approaching Irkutsk from

TABLE 4 Arithmetic Mean Isotope Composition ($\delta^{18}O$, δD, and *d* Excess), Slopes, and Intercepts of Backward Trajectory Clusters 1–4 (Each Cluster Contains *n* Single Events and % Repetitions) for Irkutsk Precipitation Events

Cluster	*n*/(%)	$\delta^{18}O$ (‰)	δD (‰)	*d* (‰)	Slope	Intercept	r^2	*p*
1	58/(20)	−20.4±9.4	−158.5±71.5	5.5±10.3	7.6	−4.2	0.98	<.001
2	96/(34)	−21.6±7.9	−166.7±62.8	6.2±7.4	7.9	4.0	0.99	<.001
3	65/(23)	−15.4±8.4	−118.5±61.2	5.1±9.6	7.2	−7.2	0.98	<.001
4	65/(23)	−19.5±10.1	−152.5±76.6	3.4±9.7	7.5	6.4	0.99	<.001

TABLE 5 Seasonal Frequencies (n Amount of Events and % Repetitions) and Mean Isotope Composition of the Backward Trajectory Clusters 1–4 Calculated for Single Precipitation Events in Irkutsk Between June 2011 and April 2017

Season	Cluster	*n*/(%)	$\delta^{18}O$ (‰)	δD (‰)	*d* (‰)
DJF	1	22/(26)	−28.0±4.6	−215.2±41.5	9.6±7.2
	2	43/(50)	−26.8±5.4	−209.0±44.2	5.5±6.6
	3	9/(10)	−28.4±6.5	−215.1±49.4	12.4±10.3
	4	12/(14)	−34.1±4.8	−269.2±36.8	5.3±6.4
	mean		−29.3±3.3	−227.1±28.2	8.2±3.5
MAM	1	12/(27)	−18.4±7.2	−146.3±60.5	2.2±10.7
	2	21/(47)	−17.2±5.6	−131.2±44.1	6.8±9.5
	3	6/(13)	−16.2±6.1	−125.9±42.2	3.8±7.8
	4	6/(13)	−14.7±4.1	−115.2±25.1	2.0±11.0
	mean		−16.6±1.6	−129.7±12.9	3.7±2.2
JJA	1	12/(13)	−6.9±2.7	−59.2±17.3	−4.1±8.6
	2	12/(13)	−12.1±2.3	−91.6±15.7	5.0±6.5
	3	34/(38)	−9.5±2.8	−75.8±20.9	0.8±8.3
	4	31/(35)	−12.1±3.4	−98.9±24.7	−2.0±7.6
	mean		−10.1±2.5	−81.4±17.6	−0.1±4.8
SON	1	12/(19)	−22.1±5.7	−166.0±42.6	10.8±9.0
	2	20/(31)	−20.7±8.4	−158.1±64.3	7.5±7.3
	3	16/(25)	−20.3±6.4	−152.2±46.8	10.5±7.8
	4	16/(25)	−24.5±8.6	−182.8±65.4	13.0±7.6
	mean		−21.9±1.9	−164.8±13.3	10.4±2.2

Abbreviations: DJF, December-January-February; JJA June-July-August; MAM: March-April-May; SON: September-October-November.

northern Siberia (cluster 4). Among four identified main directions of atmospheric moisture, two have rather long and two have relatively short distance paths (Figure 7). Precipitation events with long distance paths transported from the west (cluster 1) and northwest (cluster 2) are characterized by very similar mean isotope values of around −21‰ for $\delta^{18}O$ and −162.5‰ for δD (Table 4). However, unlike precipitation from cluster 1 (*d* excess = +5.5‰, slope = 7.6, intercept = −4.2), cluster 2 has slightly higher mean *d* excess of +6.2‰ and is situated closer to the GMWL (slope = 7.9, intercept = 4.0), which could be indicative for different moisture sources. Cluster 1 comprises air masses with moisture pathways passing over the complete continent for at least 5 days (Figure 7), which could originate from the Aral-Caspian region. In contrast, cluster 2 includes numerous air parcels originating over the Atlantic Ocean (Figure 7), thus probably with a stronger oceanic input, which could explain the difference in isotopic characteristics.

Both, clusters 3 and 4, have much shorter pathways (Figure 7) and are composed by air masses that have more local circulation patterns. Events from cluster 3 characterized by the highest mean $\delta^{18}O$ and δD values of −15.4‰ and −118.5‰, respectively (Table 4) originate west-southwest from Irkutsk, probably reflecting a local moisture source over the continent (*d* excess = +5.5‰, slope = 7.2, intercept = −7.2). Such cyclones are formed as disturbances on the polar front south 50°N over Mongolia when cold Arctic air converges with warm and wet air from the subtropics (Gustokashina, 2003; Latysheva et al., 2009; Loshchenko, 2015). However, the subtropical air masses forming over the Indian and/or the Pacific Oceans (Marchenko et al., 2012) reaching the central part of the continent lose moisture and are significantly transformed.

The oxygen isotope record of diatoms preserved in the Lake Kotokel bottom sediment (Kostrova et al., 2013, 2014, 2016) suggests that the south-easterly moisture transport played a more significant role in the Baikal region during the Early Holocene with higher-than-present summer insolation and intensified monsoon circulation. Oppositely, the westerly moisture transport was weaker in the Eurasian midlatitudes during the Early Holocene and became stronger (similar to today) during the Late Holocene (Tarasov, Bezrukova, Müller, Kostrova, & White, 2017). Although the current study, based on the

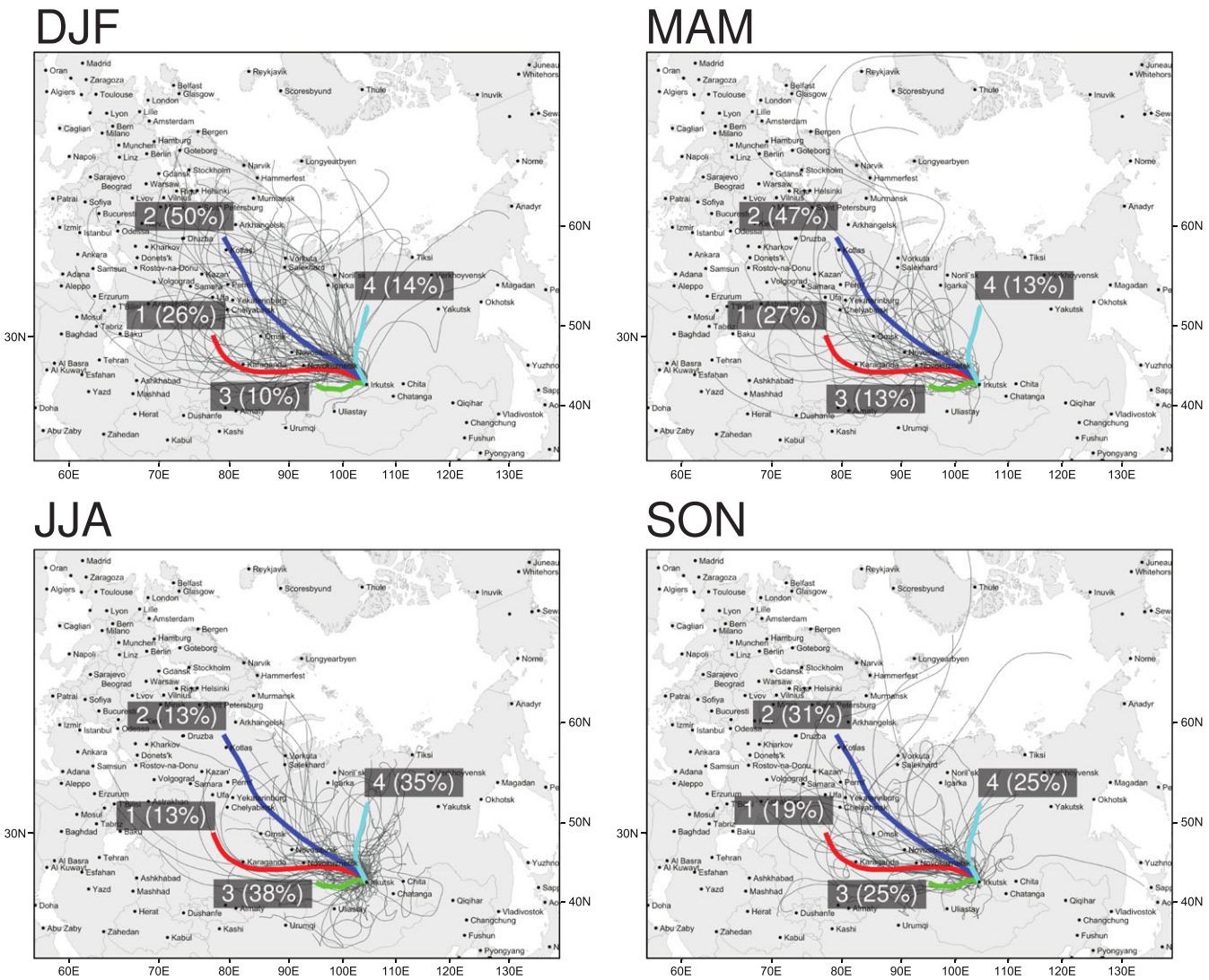

FIGURE 8 Seasonal distribution of backward trajectories for 284 single precipitation events between June 2011 and April 2017

expanded modern dataset, approves the typical "Late Holocene scenario" described in the meteorological and palaeoenvironmental publications, however, the "Early Holocene scenario" can still be traced in the stable isotope data of precipitation. This conclusion is important for future palaeoclimate reconstructions using proxy-based interpretations of the moisture origin in southeast Siberia.

Finally, cluster 4 (slope = 7.5, intercept = −6.4) mostly includes air masses with relatively light isotope composition of −19.5‰ for $\delta^{18}O$ and −152.5‰ for δD and low *d* excess = +3.4‰ (Table 4) arriving from the north. This *d* excess is in a good agreement with that for Arctic air masses (Clark & Fritz, 1997), representing local transport of moisture, probably originating from the Kara Sea and the Laptev Sea regions.

Transport of air parcels carrying water vapour that produces the precipitation at Irkutsk exhibits a strong seasonal effect (Table 5 and Figure 8), which is also reflected by the mean monthly values of the stable isotope composition of the collected samples. The seasonal distribution (Figure 8) of the clusters reveals a prevalence of western long-distance transport with oceanic contribution (cluster 2) in winter (December-January-February [DJF]; 50%), spring (March-April-May; 47%) and autumn (September-October-November; 31%) and a dominance of the continent moisture from the west-southwest (clusters 3) and of Arctic origin (cluster 4) in almost equal amount of 38% and 35%, respectively in summer (June-July-August). This migration pattern agrees with the general circulation over the Baikal region when in summer the westerly transport loses its activity and the invasions of the arctic and southern cyclones become stronger (Osipova & Osipov, 2016).

Generally, atmospheric moisture with more negative δ-values and relatively high *d* excess (Table 5) is transported to the region in winter and less negative isotopic composition and low *d* excess are typical for all clusters in summer. DJF-precipitation events with extremely low mean values of −34.1‰ for $\delta^{18}O$ and −269.2‰ for δD (*d* excess = 5.3‰) are related to cluster 4 and associated to air masses approaching from the Arctic (Figure 8). Isotopically heaviest June-July-August -precipitation with mean $\delta^{18}O$ and δD values of −6.9‰ and −59.2‰, respectively (*d* excess = −4.1‰) are linked to cluster 1 and delivered form inner continental Aral-Caspian region (Figure 8).

In summary, trajectory analysis of precipitation collected in Irkutsk from June 2011 to October 2013 and between December 2014 and April 2017 allowed the association of their isotopic composition with remote and more proximal moisture sources. Generally, our clustered backward trajectories display clear seasonal variations supported by the precipitation stable isotope signature (Figure 8 and Table 5).

6 | CONCLUSIONS

This paper presents 5 years of event-based precipitation isotopes for the city of Irkutsk (2011–2017) including its statistical characteristics, correlation with key meteorological parameters (rH, T, and P) to fill a significant gap in the Siberian precipitation isotope network. Our results distinctly differ from earlier studies for Irkutsk based on only 11 months of GNIP data. Consequently, we found (a) a significantly lower weighted mean annual isotopic composition (−19.5‰ for $\delta^{18}O$ and −150.4‰ for δD) and higher *d* excess (+6.1‰). (b) The annual isotope cycle follows the well-established cycle for mid latitudes (Rozanski et al., 1993) indicating distinct seasonal variations with higher $\delta^{18}O$ and δD values and lower *d* excess for summer precipitation and lighter isotope composition and higher *d* excess for winter air masses. (c) Air temperature is the most important control on $\delta^{18}O$ and δD strongly influenced by seasonality and explains ~85% of the variability in δ-values. The derived temperature-isotope relationships yield new, more reliable and representative coefficients of +0.50‰/°C (r^2 = 0.85; p <.01) for oxygen and +3.9‰/°C (r^2 = 0.85; p <.01) for hydrogen isotopes. This differs significantly from earlier studies with a much lower isotope-temperature relationship of +0.36‰/°C (Seal & Shanks, 1998). Moreover, the amount of precipitation and rH are obviously no key factors explaining variations in the isotope composition of Irkutsk precipitation. (d) The ECHAM5-wiso modelled monthly temperature (r^2 = 0.99; p <.01; n = 71) and weighted $\delta^{18}O$ (r^2 = 0.87; p <.01; n = 55) are in very good agreement with the measured data and might be used as alternative data sours in the region. (e) Long distance north-westerly air masses from the Atlantic Ocean (34%; $\delta^{18}O$ = −21.6‰; δD = −166.7‰; *d* excess = +5.5‰) in combination with westerly (20%; $\delta^{18}O$ = −20.4‰; δD = −158.5‰; *d* excess = +6.2‰) transport over west Siberia and northern Kazakhstan dominantly deliver precipitation during the year especially in winter, spring, and autumn. Isotopically heavy short-distance south-westerly cyclones (23%) with rather high $\delta^{18}O$ and δD values of −15.4‰ and −118.5‰, respectively (*d* excess = +5.1‰) are the most important source of summer precipitation, closely followed by isotopically lighter air masses arriving from the Arctic related to northern circulation (23%; $\delta^{18}O$ = −19.5‰; δD = −152.5‰; *d* excess = +3.4‰).

All these results have implications for isotope-based regional palaeoclimate studies, that is, those based on diatom oxygen isotopes at Lake Baikal potentially requiring a reinterpretation of earlier reconstructions.

ACKNOWLEDGMENT

This study was performed as part of the State Research Program of IGC SB RAS IX.127.1.2 from Ministry of Education and Science of the Russian Federation. It contributes to the environmental part of the international multidisciplinary project “Individual life histories in long-term culture change: Holocene hunter-gatherers in Northern Eurasia” (SSHRC Partnership Grant 895-2018-1004). We thank the German Federal Ministry of Education and Research (BMBF; grant 03G0859). We acknowledge Stefan Kruse (AWI Potsdam) for his help with boxplot illustration. We are extremely grateful to Christian Birkel and three anonymous reviewers for their constructive comments, useful suggestions and editorial corrections.

AUTHOR CONTRIBUTIONS

S. Kostrova, H. Meyer, P. Tarasov provided precipitation stable isotope data; F. Fernandoy provided HYSPLIT modelling; M. Werner provided ECHAM5-wiso simulation. All co-authors contributed to the discussion and interpretation of the data and the writing of the manuscript.

DATA AVAILABILITY STATEMENT

Data are available via the Pangaea database (www.pangaea.de).

ORCID

Svetlana S. Kostrova https://orcid.org/0000-0003-1124-5559
Hanno Meyer https://orcid.org/0000-0003-4129-4706
Francisco Fernandoy https://orcid.org/0000-0003-2252-7746
Martin Werner https://orcid.org/0000-0002-6473-0243
Pavel E. Tarasov https://orcid.org/0000-0002-7219-5009

REFERENCES

Alduchov, O. A., & Eskridge, R. E. (1996). Improved Magnus from approximation of saturation vapor pressure. *Journal of Applied Meteorology*, *35*, 601–609.

Araguás-Araguás, L., Froehlich, K., & Rozanski, K. (2000). Deuterium and oxygen-18 isotope composition of precipitation and atmospheric moisture. *Hydrological Processes*, *14*(8), 1341–1355.

Bailey, H. L., Klein, E. S., & Welker, J. M. (2019). Synoptic and mesoscale mechanisms drive winter precipitation $\delta^{18}O/\delta^{2}H$ in south-central Alaska. *Journal of Geophysical Research-Atmospheres*, *124*, 4252–4266. https://doi.org/10.1029/2018JD030050

Bezrukova, E. V., Tarasov, P. E., Solovieva, N., Krivonogov, S. K., & Riedel, F. (2010). Last glacial–interglacial vegetation and environmental dynamics in southern Siberia: Chronology, forcing and feedbacks. *Palaeogeography, Palaeoclimatology, Palaeoecology*, *296*, 185–198.

Bowen, G. J. (2008). Spatial analysis of the intra-annual variation of precipitation isotope ratios and its climatological corollaries. *Journal of Geophysical Research*, *113*, D05113. https://doi:10.1029/2007JD009295

Bowen, G. J. (2010). Statistical and geostatistical mapping of precipitation water isotope ratios. In J. West, G. Bowen, T. Dawson, & K. Tu (Eds.), *Isoscapes: Understanding movement, pattern, and process on Earth through isotope mapping* (pp. 139–160). Dordrecht Heidelberg London New York: Springer.

Bowen, G. J. (2019). The online isotopes in precipitation calculator, version 3.1. http://www.waterisotopes.org

Brázdil, R. (1992). Fluctuation of atmospheric precipitation in Europe. *GeoJournal*, *27*(3), 275–291.

Butzin, M., Werner, M., Masson-Delmotte, V., Risi, C., Frankenberg, C., Gribanov, K., … Zakharov, V. I. (2014). Variations of oxygen-18 in West Siberian precipitation during the last 50 years. *Atmospheric Chemistry and Physics*, *14*, 5853–5869. https://doi.org/10.5194/acp-14-5853-2014

Casado, M., Orsi, A. J., & Landais, A. (2017). On the limits of climate reconstruction from water stable isotopes in polar ice cores. *PAGES Magazine*, *25*(3), 146–147.

Chizhova, Y. N., Yanchenko, N. I., Budantseva, N. A., Baranov, A. N., Ruzhnikov, V. A., & Vasil'chuk, Y. K. (2016). Evaluation of the influence of Arctic and Atlantic air masses on the isotopic composition of snow cover of the city of Bratsk. *Arctic and Antarctic*, *2*, 75–85 (in Russian). http://e-notabene.ru/arctic/article_21439.html

Clark, I., & Fritz, P. (1997). *Environmental isotopes in hydrogeology* (p. 328). Boca Raton, New York: CRC Press/Lewis Publishers.

Craig, H. (1961). Isotopic variations in meteoric waters. *Science*, *133*, 1702–1703.

Danilenko, I. V., Solotchin, P. A., & Solotchina, E. P. (2015). Mineralogy of Holocene sediments of shallow lakes in the Baikal Region: A connection with paleoclimate. *Izvestiya Rossiiskoi Akademii Nauk: Seriya Geograficheskaya*, *4*, 107–112. (in Russian)

Dansgaard, W. (1964). Stable isotopes in precipitation. *Tellus*, *16*(4), 436–468.

Dee, D. P., Uppala, S. M., Simmons, A. J., Berrisford, P., Poli, P., Kobayashi, S., … Vitart, F. (2011). The ERA-Interim reanalysis: Configuration and performance of the data assimilation system. *Quarterly Journal of the Royal Meteorological Society*, *137*(656), 553–597. https://doi.org/10.1002/qj.828

Draxler, R. R., & Hess, G. D. (1998). An overview of the HYSPLIT_4 modelling system for trajectories, dispersion and deposition. *Australian Meteorological Magazine*, *47*, 295–308.

Draxler, R. R., & Rolph, G. D. (2015). *HYSPLIT (HYbrid Single-Particle Lagrangian Integrated Trajectory) model access via NOAA ARL READY website*. Silver Spring, MD: NOAA Air Resources Laboratory. https://ready.arl.noaa.gov/HYSPLIT.php

Fernandoy, F., Meyer, H., & Tonelli, M. (2012). Stable water isotopes of precipitation and firn cores from the northern Antarctic Peninsula region as a proxy for climate reconstruction. *The Cryosphere*, *6*, 313–330.

Galloway, J. N., & Cowling, E. B. (1978). The effects of precipitation on aquatic and terrestrial ecosystems: a proposed precipitation chemistry network. *Journal of the Air Pollution Control Association*, *28*(3), 229–235.

Gat, J. R. (2000). Atmospheric water balance—The isotopic perspective. *Hydrological Processes*, *14*, 1357–1369.

Gat, J. R., Mook, W. G., & Meijer, H. A. J. (2001). Atmospheric water. In *Environmental isotopes in the hydrological cycle: Principles and applications 2* (pp. 165–235). Paris: Technical Documents in Hydrology. UNESCO – IAEA.

Gryazin, V., Risi, C., Jouzel, J., Kurita, N., Worden, J., Frankenberg, C., … Stukova, O. (2014). To what extent could water isotopic measurements help us understand model biases in the water cycle over Western Siberia. *Atmospheric Chemistry and Physics*, *14*, 9807–9830. https://doi.org/10.5194/acp-14-9807-2014

Gustokashina, N. N. (2003). *Long-term changes of the main climate elements in the territory of the Pre-Baikal region* (p. 107). Irkutsk: Publishing house of the Institute of Geography SB RAS. (in Russian)

Harrison, S. P., Yu, G., & Tarasov, P. E. (1996). Late Quaternary lake-level record from northern Eurasia. *Quaternary Research*, *45*, 138–159.

IAEA/WMO (2018). Global Network of Isotopes in Precipitation. *The GNIP Database*. https://nucleus.iaea.org/wiser

Intergovernmental Panel on Climate Change (2014). *Climate Change 2014: Synthesis Report. Contribution of Working Groups I, II and III to the Fifth Assessment Report of the Intergovernmental Panel on Climate Change* [Core Writing Team, R. K. Pachauri, & L. A. Meyer (Eds.)]. IPCC, Geneva, Switzerland. 151 p.

Jouzel, J., & Merlivat, L. (1984). Deuterium and oxygen-18 in precipitation: modelling of the isotopic effects during snow formation. *Journal of Geophysical Research*, *89*, 11749–11757.

Kalmychkov, G. V., Kuz'min, M. I., Pokrovskii, B. G., & Kostrova, S. S. (2007). Oxygen isotopic composition in diatom algae frustules from Lake Baikal sediments: Annual mean temperature variations during the last 40 Ka. *Doklady Earth Sciences*, *413*(2), 206–209.

Koster, R., Jouzel, J., Suozzo, R., Russell, G., Broecker, W., Rind, D., & Eagleson, P. (1986). Global sources of local precipitation as determined by the NASA/GISS GCM. *Geophysical Research Letters*, *13*, 121–124.

Koster, R. D., de Valpine, D. P., & Jouzel, J. (1993). Continental water recycling and $H_2{}^{18}O$ concentrations. *Geophysical Research Letters*, *20*, 2215–2218.

Kostrova, S. S., Meyer, H., Chapligin, B., Kossler, A., Bezrukova, E. V., & Tarasov, P. E. (2013). Holocene oxygen isotope record of diatoms from Lake Kotokel (southern Siberia, Russia) and its palaeoclimatic implications. *Quaternary International*, *290–291*, 21–34.

Kostrova, S. S., Meyer, H., Chapligin, B., Tarasov, P. E., & Bezrukova, E. V. (2014). The last glacial maximum and late glacial environmental and climate dynamics in the Baikal region inferred from an oxygen isotope record of lacustrine diatom silica. *Quaternary International*, *348*, 25–36.

Kostrova, S. S., Meyer, H., Tarasov, P. E., Bezrukova, E. V., Chapligin, B., Kossler, A., … Kuzmin, M. I. (2016). Oxygen isotope composition of diatoms from sediments of Lake Kotokel (Buryatia). *Russian Geology and Geophysics*, *57*, 1239–1247. https://doi.org/10.1016/j.rgg.2016.08.009

Kravchinsky, V. A. (2017). Magnetostratigraphy of the Lake Baikal sediments: A unique record of 8.4 Ma of continuous sedimentation in the continental environment. *Global and Planetary Change*, *152*, 209–226.

Krklec, K., & Domínguez-Villar, D. (2014). Quantification of the impact of moisture source regions on the oxygen isotope composition of precipitation over Eagle Cave, central Spain. *Geochimica et Cosmochimica Acta*, *134*, 39–54.

Kurita, N. (2011). Origin of Arctic water vapor during the ice-growth season. *Geophysical Research Letters*, *38*, L02709. https://doi:10.1029/2010GL046064

Kurita, N., Numaguti, A., Sugimoto, A., Ichiyanagi, K., & Yoshida, N. (2003). Relationship between the variation of isotopic ratios and the source of summer precipitation in eastern Siberia. *Journal of Geophysical Research*, *108*(D11), 4339. https://doi:10.1029/2001JD001359

Kurita, N., Sugimoto, A., Fujii, Y., Fukazawa, T., Makarov, V. N., Watanabe, O., … Yoshida, N. (2005). Isotopic composition and origin of snow over Siberia. *Journal of Geophysical Research*, *110*, D13102. https://doi.org/10.1029/2004JD005053

Kurita, N., Yoshida, N., Inoue, G., & Chayanova, E. A. (2004). Modern isotope climatology of Russia: A first assessment. *Journal of Geophysical Research*, *109*, D03102. https://doi:10.1029/2003JD003404

Kuz'min, M. I., Khursevich, G. K., Prokopenko, A. A., Fedenya, S. A., & Karabanov, E. B. (2009). *Centric diatoms in Lake Baikal during the Late Cenozoic: morphology, systematics, stratigraphy and stages of development (based on the deep cores of the Baikal Drilling Project)*. Academic Publishing House "GEO", Novosibirsk. 374 p. (in Russian).

Ladeischikov, N. P. (Ed.) (1977). *Structure and resources of climate of Baikal and adjacent territories* (p. 270). Novosibirsk: Nauka. (in Russian)

Latysheva, I. V., Sinyukovich, V. N., & Chumakova, E. V. (2009). Recent peculiarities of hydrological and meteorological regime of the Lake Baikal Southern Coast. *The Bulletin of Irkutsk State University. Series Earth of Science*, *2*(2), 117–133. (in Russian)

Leonelli, G., Battipaglia, G., Cherubini, P., Saurer, M., Siegwolf, R. T. W., Maugeri, M., … Pelfini, M. (2017). Larix decidua $\delta^{18}O$ tree-ring cellulose mainly reflects the isotopic signature of winter snow in a high-altitude glacial valley of the European Alps. *Science of the Total Environment*, *579*, 230–237. https://doi.org/10.1016/j.scitotenv.2016.11.129

Leonova, G. A., Mal'tsev, A. E., Melenevskii, V. N., Miroshnichenko, L. V., Kondrat'eva, L. M., & Bobrov, V. A. (2018). Geochemistry of diagenesis of organogenic sediments: An example of small lakes in Southern West Siberia and Western Baikal Area. *Geochemistry International*, *56*(4), 344–361.

Liang, F., Brook, G. A., Kotlia, B. S., Railsback, L. B., Hardt, B., Cheng, H., … Kandasamy, S. (2015). Panigarh cave stalagmite evidence of climate change in the Indian Central Himalaya since AD 1256: Monsoon breaks and winter southern jet depressions. *Quaternary Science Reviews*, *124*, 145–161. https://doi.org/10.1016/j.quascirev.2015.07.017

Loshchenko, K. A. (2015). Pressure systems and atmospheric fronts in the territory of the Irkutsk Region in 2000–2013. *The Bulletin of Irkutsk State University. Series Earth of Science*, *12*, 50–63. (in Russian)

Lowe, P. R., & Ficke, J. M. (1974). The computation of saturation vapor pressure. *Technical paper of Environmental Prediction Research Facility Naval Postgraduate School Monterey, California*, *4–74*, 27.

Lydolph, P. E. (1977). Climates of the Soviet Union. In *World Survey of Climatology 7* (p. 443). Amsterdam-Oxford-New York: Elsevier Scientific Publishing Company.

Mackay, A. W., Bezrukova, E. V., Boyle, J. F., Holmes, J. A., Panizzo, V. N., Piotrowska, N., … White, D. (2013). Multiproxy evidence for abrupt climate change impacts on terrestrial and freshwater ecosystems in the Ol'khon region of Lake Baikal, central Asia. *Quaternary International*, *290–291*, 46–56.

Mackay, A. W., Swann, G. E. A., Brewer, T. S., Leng, M. J., Morley, D. W., Piotrowska, N., … White, D. (2011). A reassessment of late glacial—Holocene diatom oxygen isotope record from Lake Baikal using a geochemical mass-balance approach. *Journal of Quaternary Science*, *26*(6), 627–634. https://doi.org/10.1002/jqs.1484

Mackay, A. W., Swann, G. E. A., Fagel, N., Fietz, S., Leng, M. J., Morley, D., … Tarasov, P. (2013). Hydrological instability during the Last Interglacial in central Asia: a new diatom oxygen isotope record from Lake Baikal. *Quaternary Science Reviews*, *66*, 45–54. https://doi.org/10.1016/j.quascirev.2012.09.025

Malygina, N. S., Eirikh, A. N., Kurepina, N. Y., & Papina, T. S. (2019). Isotopic composition of precipitation in Altai foothills: Observation and interpolation data. *Bulletin of the Tomsk Polytechnic University: Geo Assets Engineering*, *330*(2), 44–54. (in Russian)

Marchenko, O. Y., Mordvinov, V. I., & Berezhnykh, T. V. (2012). Extreme water content of the Selenga River and features of the summer circulation of the atmosphere. *Russian Meteorology and Hydrology*, *10*, 81–93. (in Russian)

Merlivat, L., & Jouzel, J. (1979). Global climatic interpretation of the deuterium – oxygen 18 relationship for precipitation. *Journal of Geophysical Research*, *84*(C8), 5029–5033.

Meyer, H., Dereviagin, A. Y., Siegert, C., Hubberten, H.-W., & Rachold, V. (2002). Paleoclimate studies on Bykovsky Peninsula, North Siberia; hydrogen and oxygen isotopes in ground ice. *Polarforschung*, *70*, 37–51.

Meyer, H., Opel, T., Laepple, T., Dereviagin, A. Y., Hoffmann, K., & Werner, M. (2015). Long-term winter warming trend in the Siberian Arctic during the mid- to late Holocene. *Nature Geoscience*, *8*, 122–125.

Meyer, H., Schönicke, L., Wand, U., Hubberten, H.-W., & Friedrichsen, H. (2000). Isotope studies of hydrogen and oxygen in ground ice—Experiences with the equilibration technique. *Isotopes in Environmental and Health Studies*, *36*, 133–149.

Morley, D. W., Leng, M. J., Mackay, A. W., & Sloane, H. J. (2005). Late glacial and Holocene environmental change in the Lake Baikal region documented by oxygen isotopes from diatom silica. *Global and Planetary Change*, *46*, 221–233.

Numaguti, A. (1999). Origin and recycling processes of precipitating water over the Eurasian continent: Experiments using an atmospheric general circulation model. *Journal of Geophysical Research*, *104*, 1957–1972.

Osipova, O. P., & Osipov, E. Y. (2016). Atmospheric circulation mechanisms and their association with the processes of glacier meltdown of the Baikal Range. *Geography and Natural Resources*, *5*, 15–19. (in Russian)

Pang, H., Hou, S., Kaspari, S., & Mayewski, P. A. (2014). Influence of regional precipitation patterns on stable isotopes in ice cores from the central Himalayas. *The Cryosphere*, *8*, 289–301.

Papina, T. S., Malygina, N. S., Eirikh, A. N., Galanin, A. A., & Zheleznyak, M. N. (2017). Isotopic composition and sources of atmospheric precipitation in Central Yakutia. *Earth's Cryosphere*, *21*(2), 52–61.

Partin, J. W., Jenson, J. W., Banner, J. L., Quinn, T. M., Taylor, F. W., Sinclair, D., … Taboroši, D. (2012). Relationship between modern rainfall variability, cave dripwater, and stalagmite geochemistry in Guam, USA. *Geochemistry, Geophysics, Geosystems*, *13*(3), Q03013. https://doi.org/10.1029/2011GC003930

Pfahl, S., & Sodemann, H. (2014). What controls deuterium excess in global precipitation? *Climate of the Past*, *10*, 771–781.

Risi, C., Noone, D., Frankenberg, C., & Worden, J. (2013). Role of continental recycling in intraseasonal variations of continental moisture as deduced from model simulations and water vapor isotopic measurements. *Water Resources Research*, *49*, 4136–4156.

Roeckner, E., Brokopf, R., Esch, M., Giorgetta, M., Hagemann, S., Kornblueh, L., … Schulzweida, U. (2006). Sensitivity of simulated climate to horizontal and vertical resolution in the ECHAM5 atmosphere model. *Journal of Climate*, *19*(16), 3771–3791. https://doi.org/10.1175/JCLI3824.1

Rozanski, K., Araguás-Araguás, L., & Gonfiantini, R. (1993). Isotopic patterns in modern global precipitation. Geophysical Monograph 78. In *Climate Change in Continental Isotope Records* (pp. 1–36). Washington: American Geophysical Union Monograph.

Rozanski, K., Johnsen, S. J., Schotterer, U., & Thompson, L. G. (1997). Reconstruction of past climates from stable isotope records of palaeoprecipitation preserved in continental archives. *Hydrological Sciences Journal*, *42*, 725–745.

Sánchez-Murillo, R., Durán-Quesada, A. M., Birkel, C., Esquivel-Hernández, G., & Boll, J. (2017). Tropical precipitation anomalies and *d*-excess evolution during El Niño 2014-16. *Hydrological Processes*, *31*, 956–967.

Seal, R. R., & Shanks, W. C. (1998). Oxygen and hydrogen isotope systematics of Lake Baikal, Siberia: implications for paleoclimate studies. *Limnology and Oceanography*, *43*, 1251–1261.

Shimaraev, M. N., Verbolov, V. I., Granin, N. G., & Sherstyankin, P. P. (1994). *Physical Limnology of Lake Baikal: a Review* (p. 81). Irkutsk, Irkutsk-Okayama: Baikal International Center of Ecological Research.

Shver, T. A., & Formanchuk, N. P. (Eds.) (1981). *Climate of Irkutsk* (p. 246). Leningrad: Gidrometeoizdat. (in Russian)

Sklyarov, E. V., Solotchina, E. P., Vologina, E. G., Ignatova, N. V., Izokh, O. P., Kulagina, N. V., … Khlystov, O. M. (2010). Detailed Holocene climate record from the carbonate section of saline Lake Tsagan-Tyrm (West Baikal area). *Russian Geology and Geophysics*, *51*(3), 237–258. https://doi.org/10.1016/j.rgg.2010.02.001

Stein, A. F., Draxler, R. R., Rolph, G. D., Stunder, B. J. B., Cohen, M. D., & Ngan, F. (2015). NOAA's HYSPLIT atmospheric transport and dispersion modeling system. *Bulletin of the American Meteorological Society*, *96*, 2059–2077.

Stewart, M. K. (1975). Stable isotope fractionation due to evaporation and isotopic exchange of falling waterdrops: Applications to atmospheric processes and evaporation of lakes. *Journal of Geophysical Research*, *80*(9), 1133–1146.

Swann, G. E. A., Mackay, A. W., Vologina, E., Jones, M. D., Panizzo, V. N., Leng, M. J., … Sturm, M. (2018). Lake Baikal isotope records of Holocene Central Asian precipitation. *Quaternary Science Reviews*, *189*, 210–222. https://doi.org/10.1016/j.quascirev.2018.04.013

Tang, Y., Song, X., Zhang, Y., Han, D., Ai, L., Zhao, T., & Wang, Y. (2017). Using stable isotopes to understand seasonal and interannual dynamics in moisture sources and atmospheric circulation in precipitation. *Hydrological Processes*, *31*, 4682–4692.

Tarasov, P. E., Bezrukova, E. V., Müller, S., Kostrova, S. S., & White, D. (2017). Chapter 2: Climate and Vegetation History. In R. J. Losey, & T. Nomokonova (Eds.), *Holocene Zooarchaeology of Cis-Baikal* (pp. 15–26). Mainz: Archaeology in China and East Asia 6. Nünnerich–Asmus Verlag & Media GmbH.

Tarasov, P. E., Ilyashuk, B. P., Leipe, C., Müller, S., Plessen, B., Hoelzmann, P., … Meyer, H. (2019). Insight into the Last Glacial Maximum climate and environments of the Baikal region. *Boreas*, *48*, 488–506. https://doi.org/10.1111/bor.12330

Trenberth, K. E. (2011). Changes in precipitation with climate change. *Climate Research*, *47*, 123–138.

Ueta, A., Sugimoto, A., Iijima, Y., Yabuki, H., & Maximov, T. C. (2014). Contribution of transpiration to the atmospheric moisture in eastern Siberia estimated with isotopic composition of water vapour. *Ecohydrology*, *7*(2), 197–208.

Ueta, A., Sugimoto, A., Iijima, Y., Yabuki, H., Maximov, T. C., Velivetskaya, T. A., & Ignatiev, A. V. (2013). Factors controlling diurnal variation in the isotopic composition of atmospheric water vapour observed in the taiga, eastern Siberia. *Hydrological Processes*, *27*, 2295–2305.

van Hardenbroek, M., Chakraborty, A., Davies, K. L., Harding, P., Heiri, O., Henderson, A. C. G., … Wooller, M. J. (2018). The stable isotope composition of organic and inorganic fossils in lake sediment records: Current understanding, challenges, and future directions. *Quaternary Science Reviews*, *196*, 154–176. https://doi.org/10.1016/j.quascirev.2018.08.003

Wei, Z., Lee, X., Liu, Z., Seeboonruang, U., & Koike, M. (2018). Influences of large-scale convection and moisture source on monthly precipitation isotope ratios observed in Thailand, Southern Asia. *Earth and Planetary Science Letters*, *488*, 181–192.

Werner, M., Langebroek, P. M., Carlsen, T., Herold, M., & Lohmann, G. (2011). Stable water isotopes in the ECHAM5 general circulation model: Toward high-resolution isotope modeling on a global scale. *Journal of Geophysical Research-Atmospheres*, *116*, D15109.

Wu, H., Zhang, X., Xiaoyan, L., Li, G., & Huang, Y. (2015). Seasonal variations of deuterium and oxygen-18 isotopes and their response to moisture source for precipitation events in the subtropical monsoon region. *Hydrological Processes*, *29*, 90–102.

Yang, Y., Wu, Q., Hou, Y., Zhang, P., Yun, H., Jin, H., … Jiang, G. (2019). Using stable isotopes to illuminate thermokarst lake hydrology in permafrost regions on the Qinghai-Tibet plateau, China. *Permafrost and Periglacial Processes*, *30*, 58–71. https://doi.org/10.1002/ppp.1996

Yao, T., Masson-Delmotte, V., Gao, J., Yu, W., Yang, X., Risi, C., … Hou, S. (2013). A review of climatic controls on $\delta^{18}O$ in precipitation over the Tibetan Plateau: Observations and simulations. *Reviews of Geophysics*, *51*, 525–548. https://doi.org/10.1002/rog.20023

Yurtsever, Y., & Gat, J. R. (1981). Atmospheric waters. In J. R. Gat, & R. Gonfiantini (Eds.), *Stable isotope hydrology: Deuterium and oxygen-18 in the water cycle* (Vol. 210) (pp. 103–142). Vienna: IAEA Technical Report Series.

SUPPORTING INFORMATION

Additional supporting information may be found online in the Supporting Information section at the end of this article.

How to cite this article: Kostrova SS, Meyer H, Fernandoy F, Werner M, Tarasov PE. Moisture origin and stable isotope characteristics of precipitation in southeast Siberia. *Hydrological Processes*. 2019;1–17. https://doi.org/10.1002/hyp.13571